Nanoscale Advances

ROYAL SOCIETY OF CHEMISTRY

PAPER

View Article Online
View Journal | View Issue

Check for updates

Cite this: *Nanoscale Adv.*, 2020, **2**, 1301

Electrospinning chiral fluorescent nanofibers from helical polyacetylene: preparation and enantioselective recognition ability†

Jiali Yang,[ab] Pengpeng Li,[ab] Biao Zhao,[b] Kai Pan *[b] and Jianping Deng *[ab]

Received 23rd December 2019
Accepted 20th February 2020

DOI: 10.1039/d0na00127a

rsc.li/nanoscale-advances

Chirality is ubiquitous in nature and closely related to the pharmacological effects of chiral drugs. Therefore, chiral recognition of molecular enantiomers becomes an important research theme. Fluorescence detection is highly sensitive and fast but has achieved only limited success in enantiomeric detection due to the lack of powerful chiral fluorescence detection materials. In this paper, a novel chiral fluorescent probe material, *i.e.* a chiral fluorescent nanofiber membrane, is prepared from chiral helical substituted polyacetylene by the electrospinning technique. The SEM images demonstrate the success in fabricating continuous, uniform nanofibers with a diameter of about 100 nm. Circular dichroism spectra show that the nanofibers exhibit fascinating optical activity. One of the enantiomeric chiral fluorescent membranes has chiral fluorescence recognition effects towards alanine and chiral phenylethylamine, while the other enantiomeric membrane does not. The prepared chiral fluorescent nano-materials are expected to find various applications in chirality-related fields due to their advantages such as chirality, fluorescence, and a high specific surface area. The established preparation approach also promises a potent and versatile platform for developing advanced nanofiber materials from conjugated polymers.

Open Access Article. Published on 21 Februarie 2020. Downloaded on 2026-04-27 11:59:08 nm..
This article is licensed under a Creative Commons Attribution-NonCommercial 3.0 Unported Licence.

1. Introduction

Chirality is a basic feature of nature. Its importance has been widely recognized, in particular when designing and developing new pharmaceutical compounds.[1–6] The handedness of enantiomeric drugs greatly influences their pharmacological effects.[7–10] One enantiomeric drug may exhibit beneficial effects while the other one exhibits inactivity or even toxicity. Therefore, the recognition of chiral enantiomers is of essential significance for drugs associated with chirality.[11,12] To date, various enantioselective recognition systems have been extensively developed, majorly based on natural chiral (macro) molecules and synthetic chiral (macro)molecules.[13,14] Chiral recognition also plays important roles in other cases involving chirality, such as crystal growth, enantiomeric separation, and self-assembly.[15] In recent years, chiral recognition research has made great progress, and various methods have been established for chiral recognition/resolution,[16–21] *e.g.*, using spectroscopy, chromatography, and sensors.[22,23] These routine approaches frequently show the disadvantages of complicated instrumentation and high cost. To overcome the limitations, using fluorescence technology for chiral recognition may be a good choice due to its obvious advantages.[24] On the other hand, diverse chiral fluorescent helical polymers have been synthesized and some demonstrate excellent chiral recognition capability.[25–29] Nonetheless, to the best of our knowledge, there have been no reports on preparing continuous, chiral fluorescent nanofibers from chiral helical polymers. We hypothesize that the as-designed chiral fluorescent nanofibers, in particular those constructed from chiral helical polymers, may show obvious advantages when used as chiral materials.

Fluorescence technology plays an important role in many significant fields such as diagnostics, imaging, and detection, helping us understand the causes of disease, personalized medicine and the mysteries of life.[30,31] Recently, fluorescence technology has witnessed significant progress in examining enantiomeric compositions.[32,33] For instance, fluorescent probes have attracted much attention due to their high sensitivity, rapidity, and safety in fluorescence analysis.[34–36] In theory, a fluorescent substance with chiral recognition capacity, especially those from chiral helical polymers showing chiral amplification effects,[37–41] shall provide promising chiral fluorescent materials. In our previous work, chiral fluorescent nanoparticles were prepared.[42] To fully explore the potential uses of chiral fluorescent polymers, we in the present work designed and prepared chiral fluorescent nanofibers derived from polymers by electrospinning. The as-fabricated nanofibers

[a]*State Key Laboratory of Chemical Resource Engineering, Beijing University of Chemical Technology, Beijing 100029, China. E-mail: dengjp@mail.buct.edu.cn*

[b]*College of Materials Science and Engineering, Beijing University of Chemical Technology, Beijing 100029, China*

† Electronic supplementary information (ESI) available: Structural formula, FT-IR spectra, GPC, electrospinning parameters, SEM images, digital photo of fluorescent polymer membranes, CD and UV-vis absorption spectra, and fluorescence emission spectra. See DOI: 10.1039/d0na00127a

Open Access Article. Published on 21 Februarie 2020. Downloaded on 2026-04-27 11:59:08 nm..
This article is licensed under a Creative Commons Attribution-NonCommercial 3.0 Unported Licence.

show interesting chiral fluorescence recognition ability, as reported below.

Nowadays, the major methods for preparing polymeric nanofibers include stretching, microphase separation, template polymerization, self-assembly, vapor deposition, and electrospinning. Compared with other methods, electrospinning can produce continuous nanofibers by a simple process.[43–45] The prepared nanofibers have a diameter of between 50 and 1000 nm, and functional substances can also be added into the electrospinning solution for preparing functional nanofiber materials. The electrospun nanofibers have the advantages of a high specific surface area and good fiber continuity. The nanofibers have found a wide range of applications in various fields such as filtration, separation, sound absorption, energy, biomedicine, tissue engineering, and sensors.[43,46–53] Unfortunately, constructing continuous nanofibers from conjugated chiral helical polymers still remains a great academic challenge due to their inherent rigid structures. In the above context, we in the present study designed and prepared chiral fluorescent polymer nanofibers by electrospinning technology. Compared with previous nanoparticles,[42] the operation process for fabricating electrospun nanofibers is simpler; the latter also shows the advantages of mass production. The nanofibers demonstrate chiral fluorescence recognition ability towards chiral amine enantiomers (chiral phenylethylamine as a model) and chiral amino acid (alanine as a model) enantiomers, as illustratively outlined in Scheme 1. Accordingly, based on the present study, novel chiral fluorescent probes having enantioselective recognition ability can be expected in future studies.

2. Experimental

2.1 Materials

(nbd)$Rh^+B^-(C_6H_5)_4$ (nbd = 2,5-norbornadiene) was synthesized according to the procedure reported earlier.[54] Monomers L-CMF, D-CMF, and MF (as shown in Fig. S1; † the corresponding polymers are shown in Scheme 1) were synthesized by referring to the previous study.[42] L- and D-alanine, and (*R*)-(+)- and (*S*)-(−)-1-phenylethylamine (PEA) were purchased from Aladdin Reagent Co. (Shanghai, China). (*R*)-α-pinene and (*S*)-α-pinene were purchased from TCI (Shanghai) Development Co., Ltd. All the reagents above were used as received without further purification. Polyacrylonitrile (PAN, M_w = 150 000) was purchased from Shanghai Maclean Biochemical Technology Co., Ltd. Chloroform ($CHCl_3$) and *N*,*N*-dimethylformamide (DMF) (analytical grade) were purchased from Beijing Chemical Reagents Company (China) and were distilled under reduced pressure before use.

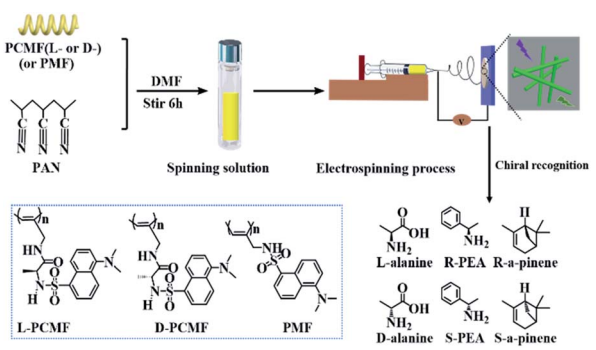

Scheme 1 Schematic illustration of the preparation of chiral fluorescent polyacetylene nanofibers and chiral recognition.

2.2 Measurements

Circular dichroism (CD) and UV-vis absorption spectra were obtained on a Jasco-810 spectropolarimeter. Fluorescence spectra were measured on a Varian Cary Eclipse spectrophotometer (Varian, USA). The morphology of the samples was observed with a Hitachi S-4800 scanning electron microscope (SEM). The molecular weights and molecular weight polydispersity (M_w/M_n) were determined by GPC/SEC (Agilent Technologies 1200 series) with THF as the eluent. Fourier transform infrared (FT-IR) spectra were recorded with a Nicolet NEXUS 670 spectrophotometer (KBr tablet).

2.3 Preparation of chiral fluorescent polyacetylenes

The chiral fluorescent polyacetylenes L-PCMF (Scheme 1) were prepared by a typical solution polymerization strategy. The chiral alkyne monomer abbreviated as L-CMF (0.36 g, 1 mmol) and (nbd)$Rh^+B^-(C_6H_5)_4$ (5.2 mg, 0.01 mmol) were dissolved in chloroform (5 mL). The polymerization was carried out under N_2 at 30 °C for 6 h. The reaction mixture was poured into a large amount of *n*-hexane (approximately 70 mL) to precipitate out the resulting polymer. After filtration, the solvent was removed by evaporation, obtaining the product. Similar solution polymerization was performed for preparing D-PCMF and PMF. Related data for the polymers are listed in Table S1.†

2.4 Electrospinning of nanofiber membranes

L-PCMF (4.6 wt%, 0.10 g) and PAN (7.4 wt%, 0.16 g) were dissolved in DMF (2 mL) by stirring at room temperature for 6 h. The resulting solution was loaded into a syringe pump. A sheet of aluminum foil was used as the collector. The distance between the needle tip and collector was 15 cm, and the voltage was set as 10 kV. The viscous solution was delivered at a fixed rate of 0.002 mL min^{-1}. The metal needle inner diameter was 0.5 mm. The temperature was 25 °C, and the humidity was 30% RH. The electrospinning time was 8 h. The electrospun fibrous mats were kept in a vacuum overnight at 45 °C to remove the residual solvent. D-PCMF- and PMF-derived nanofibers were prepared in the same way.

2.5 Chiral recognition experiments

The fluorescent polymer membrane was cut into circles of the same shape and size (diameter of 1 cm). Solutions of enantiomers with appropriate concentration were prepared (the solvent for alanine is water; and the solvent for phenethylamine and pinene enantiomers is toluene). The solutions were separately added dropwise onto the nanofiber membrane samples, which were then placed under ambient conditions for 24 h. The

 This journal is © The Royal Society of Chemistry 2020

Open Access Article. Published on 21 Februarie 2020. Downloaded on 2026-04-27 11:59:08 nm..
This article is licensed under a Creative Commons Attribution-NonCommercial 3.0 Unported Licence.

membrane samples bearing a certain chiral enantiomer were subsequently subjected to CD, UV-vis absorption, and fluorescence emission spectral measurements.

3. Results and discussion

3.1 Synthesis and characterization of chiral fluorescent nanofibers

Referring to the previous research,[42] we successfully synthesized chiral fluorescent monomers (L-CMF and D-CMF), an achiral fluorescent monomer (MF), and their corresponding polymers (L-PCMF, D-PCMF and PMF). The obtained monomers and polymers were identified by FT-IR spectroscopy, as shown in Fig. S2.† The characteristic peaks at 2120 (C≡C), 1655 and 1568 (amide), 1323 (S=O), and 1143 cm^{-1} (C–N) demonstrate the successful obtainment of the monomers (taking L-CMF as the example). For the corresponding polymer, the C≡C bond (2120 cm^{-1}) disappeared. For the achiral monomer MF and its polymer PMF, similar results were observed. The characteristic peaks at 2120 (C≡C), 1143 (–C–N–), and 1326 cm^{-1} (–S=O–) are clearly observed in the spectrum for the achiral monomer (MF), and its corresponding polymer does not show a peak at 2120 cm^{-1} (C≡C) either. The obtained acetylenic polymers were subjected to GPC measurements to determine their molecular weight and molecular weight distribution, as listed in Table S1.† The obtained polymers have a moderate number-average molecular weight (M_n) and narrow molecular weight distribution (M_w/M_n). The results convincingly confirm the successful preparation of acetylenic polymers.

PCMF (D- and L-PCMF) solutions were subjected to electrospinning, but spherical particles with a diameter of about several hundred nanometers were obtained. Moreover, the as-produced samples were macroscopic loosely-gathered particles, as shown in Fig. S3.† Due to the rigid conjugated structure of substituted polyacetylenes, the polymers' solubility in common solvents is too low to meet the requirement for electrospinning continuous nanofibers. As a consequence, particles rather than nanofibers were obtained. Considering that the major target of the present study is to fabricate electrospun nanofibers, PAN was thus used as a support material in the subsequent experiments for electrospinning acetylenic polymers, by which continuous nanofibers (composite nanofiber membranes) were efficiently prepared. The composite membranes are soft and can be peeled off safely from the collector. The optimal electrospinning conditions were experimentally established (Table S2†). Under the optimized conditions, the solution mixtures of acetylenic polymer/PAN were electrospun. The obtained composite nanofibers were characterized by SEM (Fig. 1). It can be seen that all three types of polymeric nanofibers are randomly oriented, but they show a uniform and smooth morphology without bead formation. The diameter of the nanofibers is about 100 nm, and the individual fibers have the desirable continuity. From the SEM images, we can also find that the nanofiber membranes have a network structure, in which the fibers are intertwined like spiders' web.

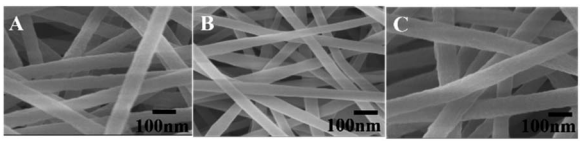

Fig. 1 SEM images of electrospun nanofibers prepared using different fluorescent polyacetylene (4.6 wt%) and PAN (7.4 wt%) mixtures in DMF solvent: (A) L-PCMF; (B) D-PCMF; and (C) PMF for detailed electrospinning parameters, see Table S2.†

The typical digital photographs of the obtained composite nanofiber membrane containing polymer L-PCMF are shown in Fig. 2. The obtained fluorescent membrane is shown under daylight (Fig. 2A) and under a 365 nm UV lamp (Fig. 2B). From the images, the fluorescence of the obtained polymer membrane seems to be green. Fig. S4† presents the membranes derived from D-PCMF and PMF under sunlight and under the 365 nm ultraviolet lamp. Their fluorescence colors are also green. We can further confirm the above observations in color by measuring the fluorescence emission spectrum of the electrospun membranes, as illustrated in Fig. 2C. The fluorescence emission spectra of the three composite membranes were measured under 365 nm excitation light. All three fluorescent membranes show strong green emission with a maximum around 500 nm.

The polymers derived from the monomer MF (including chiral and achiral MF) have been known to form helical structures.[42] The helical structures of the polymers and the optical activity can be characterized by circular dichroism (CD) and UV-vis absorption spectroscopy, as shown in Fig. 3. CD and UV-vis spectroscopy techniques have been widely used to explore the helical structures of polymers and the optical activity of the nano- and micro-materials thereof.[29,41,55] First, we measured the polymer solutions (without PAN) and the obtained CD spectra are presented in Fig. 3A. The CD signals of polymers L-PCMF and D-PCMF are symmetric; they also have the same intensity. Achiral polymer PMF has no CD signal. It can be seen from the UV-vis absorption spectra (Fig. 3A) that the absorption peaks of the three fluorescent polymers are all at about 335 nm, keeping consistent with the corresponding CD signals. According to Fig. 3A and with reference to previous studies dealing with mono-substituted polyacetylenes,[20,42] the CD signals of the chiral polymers (L-PCMF and D-PCMF) originate from the helical polymer structures with predominant helicity. For the achiral

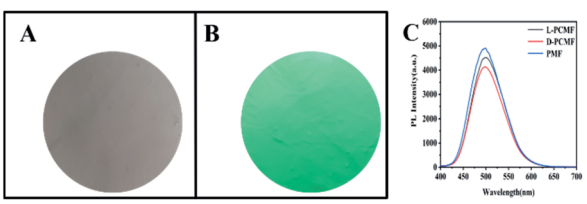

Fig. 2 Digital photos of the L-PCMF fluorescent polymer nanofiber membrane: (A) the membrane under sunlight; (B) the membrane under UV light of 365 nm; (C) fluorescence emission spectra of the three fluorescent polymer membranes (365 nm excitation).

Open Access Article. Published on 21 Februarie 2020. Downloaded on 2026-04-27 11:59:08 nm..
This article is licensed under a Creative Commons Attribution-NonCommercial 3.0 Unported Licence.

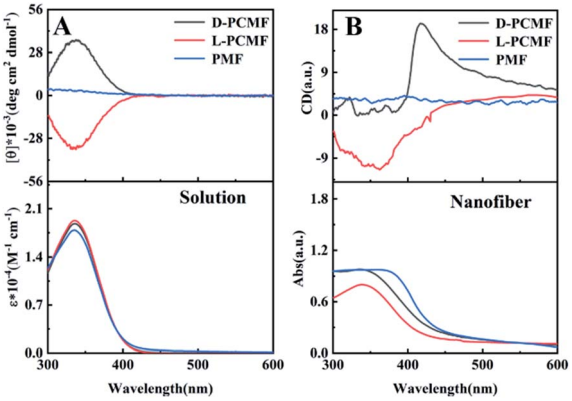

Fig. 3 CD and UV-vis absorption spectra of fluorescent polymers: (A) the spectra were measured in $CHCl_3$ solution, and the concentration of the samples was 0.25 mM; (B) the spectra were qualitatively measured using electrospun nanofiber membranes infiltrated with toluene (a drop of toluene added on a circular membrane with a diameter of 1 cm). All the spectra were measured at room temperature.

polymer (PMF), it formed racemic helical structures and thus no CD signal appeared in the CD spectrum.[40–42] Therefore we successfully prepared optically active helical polymers, L-PCMF and D-PCMF, and the optically inactive helical polymer PMF.

As mentioned above, we added PAN as a support and obtained satisfactory electrospun composite nanofiber membranes. The as-fabricated composite membranes were also characterized by CD and UV-vis absorption spectroscopy. For this purpose, the membranes were tested by using samples infiltrated with toluene to avoid damage of the morphology and structure of the nanofibers (after infiltrating with toluene, the nanofiber membranes became somewhat transparent). The recorded spectra are shown in Fig. 3B. Herein, it is important to point out that CD and UV-vis absorption spectra of substituted polyacetylenes can be quantitatively measured in solution, but for the electrospun nanofiber membranes, they can be only qualitatively characterized even when using solvent-infiltrated samples. In addition, because the thickness and homogeneity of the samples cannot be exactly controlled, the thus-recorded spectra reasonably show certain deviations. In Fig. 3B, the CD signal of the membrane D-PCMF appeared at about 420 nm, but for membrane L-PCMF, the CD signal appeared around 360 nm. In the solution state (Fig. 3A), the CD signals of the two polymers are symmetrical. However, in Fig. 3B, the CD signals of the enantiomeric polymer membranes become asymmetric. Moreover, the CD signals of both L-PCMF and D-PCMF show certain red-shifts, when compared to the corresponding CD signals measured in solution. For the nanofibers, CD spectra were also recorded by rotating the membrane samples at varying angles. The results confirm that there is no linear dichroism (LD) effect. To summarize, the electrospun nanofiber membranes showed CD signals significantly different from those of the polymer solutions.

Based on the results, we consider that in the case of the electrospun samples, the polymer chains are most likely affected by the electric field force during the electrospinning process, and the effective conjugation length of the polymer chains becomes elongated. These effects result in increased helical pitches of the polymer chains, thereby leading to red-shifts as observed in Fig. 3B. Nonetheless, the exact reasons for the fascinating phenomena, including the asymmetric CD signals occurring between L-PCMF and D-PCMF, still need to be explored in depth. We will continue our efforts along the direction to elucidate the intriguing phenomena. In summary, we successfully prepared chiral fluorescent nanofiber membranes L-PCMF and D-PCMF, as well as the achiral fluorescent nanofiber membrane PMF. With the nanofiber membranes (L-PCMF, D-PCMF and PMF) in hand, we next examined their chiral fluorescence recognition ability.

3.2 Chiral recognition ability of the electrospun nanofiber membranes

The specific experimental operating procedures are detailed in the experimental part. We qualitatively measured CD and UV-vis absorption spectra of the membranes in the presence of chiral enantiomers, aiming at exploring whether the addition of chiral small molecule enantiomers affects the helical structure of polymers constituting the membrane. The relevant results are presented in Fig. 4, taking alanine as the representative of chiral amino acids. When the enantiomeric alanine was dropped onto the membranes, the CD spectra of the chiral fluorescent membranes changed little, as shown in Fig. 4A. We also measured the CD spectra of the membranes using chiral phenethylamine and pinene enantiomers instead of alanine. No noticeable change was observed in the CD effects either (Fig. S5A and B†). Negligible changes in the spectra should be due to sample preparation and experimental errors during the testing process. Next, we also used the achiral polymer membrane (PMF) to conduct the same measurements. The PMF membrane did not exhibit changes in CD signals, as shown in Fig. 4B, S5C and D.† The racemic helical polymers constituting PMF membranes also failed to detect the chiral enantiomers. In all the recorded CD spectra, the CD signals of the added chiral small molecules cannot be observed clearly. The reasons for this

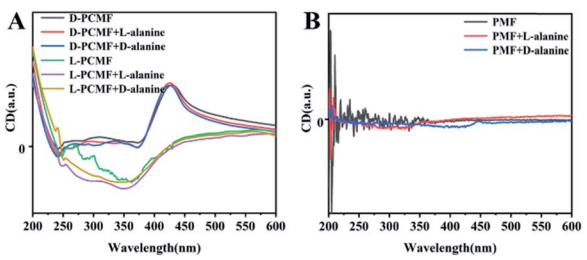

Fig. 4 CD absorption spectra of fluorescent membranes before and after addition of small molecule alanine enantiomers: (A) CD absorption spectra of chiral fluorescent membranes before and after addition of alanine enantiomers; (B) circular dichroic absorption spectra of achiral fluorescent membranes before and after addition of alanine enantiomers; a qualitative test of the electrospinning membranes that are infiltrated with toluene; a drop of toluene added on a circular electrospinning membrane sample with a diameter of 1 cm.

 This journal is © The Royal Society of Chemistry 2020

Open Access Article. Published on 21 Februarie 2020. Downloaded on 2026-04-27 11:59:08 nm..
This article is licensed under a Creative Commons Attribution-NonCommercial 3.0 Unported Licence.

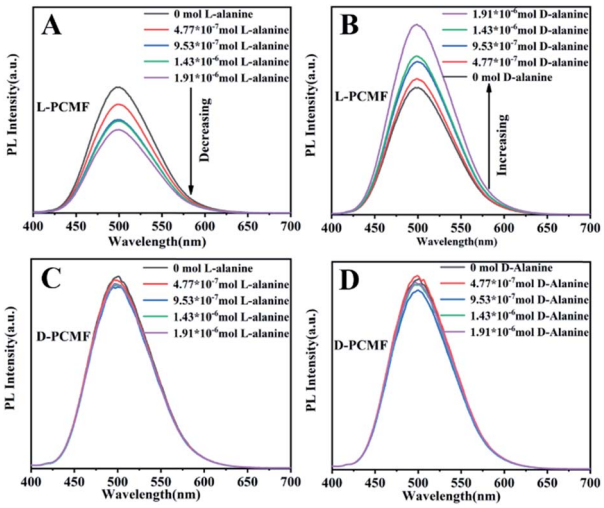

Fig. 5 Fluorescence emission spectra of the nanofibers upon recognizing chiral alanine enantiomers: (A) recognition of L-alanine using L-PCMF; (B) recognition of D-alanine using L-PCMF; (C) recognition of L-alanine using D-PCMF; (D) recognition of D-alanine using D-PCMF.

result should be the little amount of such enantiomers added; additionally, their CD signals may be overlapped by the CD signals of the polymer membranes.

The UV-vis absorption spectra of the membranes were also recorded, taking the sample containing one alanine enantiomer as the representative (Fig. S6A and B†). The addition of small molecule enantiomers has little effect on the UV-vis absorption signal. The results stated above together demonstrate that the nanofiber membranes cannot recognize enantiomers by means of CD spectral measurements. Fortunately, the membranes show the desired recognizing ability towards enantiomers in terms of fluorescence emission, as discussed in more detail below.

The addition of different amounts of enantiomers onto the fluorescent membrane of the same size was tested by fluorescent spectroscopy, as presented in Fig. 5. As the amount of D-alanine increases, the fluorescent photoluminescence (PL) intensity of the fluorescent membrane L-PCMF gradually increases. In contrast, as the added amount of L-alanine increases, the fluorescence intensity of the membrane L-PCMF gradually decreases. For the D-PCMF fluorescent membrane, an increase in the amount of D- or L-alanine failed to cause a change in the fluorescence intensity. Fig. S7† clearly presents the changing tendency of L-PCMF membrane fluorescence upon increasing the amount of enantiomeric molecules. Accordingly, the L-PCMF membrane possesses the anticipated enantioselective recognition ability; that is, the L-PCMF membrane can recognize chiral alanine. For the D-PCMF membrane, it failed to show such a recognizing ability. In order to understand more about the chiral fluorescent membranes, we further carried out a recognition experiment of the membranes towards enantiomeric phenylethylamine.

As shown in Fig. S8,† fluorescence recognition towards phenylethylamine enantiomers gave similar results. As the amount of *R*-phenylethylamine increases, the fluorescence intensity of the L-PCMF membrane gradually decreases. An increase in the *S*-phenylethylamine amount led to increased fluorescence. As far as the D-PCMF membrane is concerned, it failed to recognize *R*- and *S*-phenylethylamine. The changing tendency of L-PCMF membrane fluorescence towards chiral phenylethylamide is illustrated in Fig. S9.†

To elucidate the mechanism of fluorescence recognition, we conducted another experiment, *i.e.* the fluorescence recognition of the nanofibers towards pinene enantiomers. The experimental results are shown in Fig. S10.† We can clearly see that the fluorescence recognition towards pinene enantiomers is unsuccessful, whether using L- or D-PCMF. Specifically, the fluorescence intensity of the two chiral fluorescent membranes does not change substantially as the amount of pinene enantiomers increases. As a control experiment, the fluorescence spectra of the achiral fluorescent polymer membrane (PMF) for the recognition of the three enantiomers are shown in Fig. 6. The small molecule enantiomers added onto this membrane did not substantially change the fluorescence intensity of the membrane.

3.3 Chiral recognition mechanism

We next explored the chiral recognition mechanism of the newly prepared chiral fluorescent nanofiber membranes, on the basis of the experimental results obtained above. The changes in fluorescence spectra aforementioned are summarized in Table 1. D-PCMF and PMF membranes have no fluorescence recognition for chiral small molecules examined in this study, while the L-PCMF membrane exhibits a fluorescence

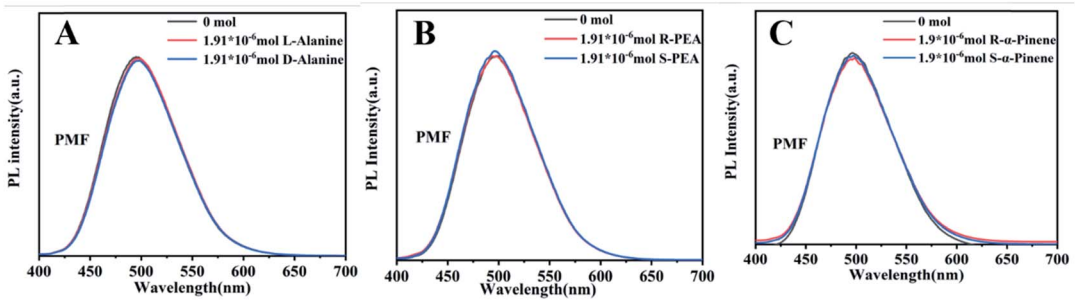

Fig. 6 Fluorescence emission spectra of PMF towards chiral enantiomers: (A) alanine; (B) phenylethylamine; (C) pinene.

Open Access Article. Published on 21 Februarie 2020. Downloaded on 2026-04-27 11:59:08 nm..
This article is licensed under a Creative Commons Attribution-NonCommercial 3.0 Unported Licence.

Table 1 Fluorescence intensity of the nanofiber membrane changing with increasing amount of enantiomers added per unit volume of fluorescent membrane[a]

	D-alanine	L-alanine	*R*-PEA	*S*-PEA	*R*-α-pinene	*S*-α-pinene
L-PCMF	↑	↓	↓	↑	—	—
D-PCMF	—	—	—	—	—	—
PMF	—	—	—	—	—	—

[a] ↑ PL intensity increasing, ↓ PL intensity decreasing, and — PL intensity unchanging.

recognition effect on them, *i.e.*, alanine and phenethylamine enantiomers. However, as far as the nonpolar pinene is concerned, no chiral recognition was observed. In addition, there is no significant change in the CD signal accompanying the change in fluorescence, which has been discussed above. One possible mechanism for the fluorescence recognition is illustratively shown in Scheme 2.

By comparing chiral fluorescent membranes (PCMF) with achiral fluorescent membranes (PMF), we find that chirality (originating from chiral helical polymer chains) plays an important role in enantiomeric recognition. If the fluorescent membrane does not have chirality (the case of PMF), the fluorescent membrane does not show chiral recognition ability. A possible reason for this observation lies in that polymer chains with different conformations (optically active helices *vs.* optically inactive helices) have varied chiral spatial configurations. When chiral small molecules are encountered, the chiral small molecules with a suitable stereo-structure will interact with the chiral polymer chains. Therefore, the chirality of small molecules affects the secondary structure of the polymer chains forming the membrane. At the same time, the combination with small molecules also affects the electron cloud distribution of the polymer chains, thereby affecting the fluorescence intensity of the polymeric membrane. If the fluorescent polymer chains are achiral, the chiral enantiomers act in the same way on the achiral polymers. Accordingly, the achiral polymers fail to show chiral recognition ability.

In the chiral fluorescent membranes, the L-PCMF membrane demonstrates chiral recognition ability but shows little change in both the position and intensity of the CD signals during the chiral recognition process. Herein we propose a possible explanation for this interesting observation. A double-layered hydrogen bond structure is formed surrounding the polymer backbones, as illustratively shown in Scheme 2. In the course of chiral recognition, the inner hydrogen bonds keep unaffected, while the outer hydrogen bonds are destroyed because of the added chiral small molecules (enantiomers). Therefore, the CD signal of the polymer chains does not change, but the fluorescence spectrum intensity changes.

As shown in Scheme 2A, when the small molecules (L-alanine and *R*-PEA) disrupt the external hydrogen bonds of adjacent side groups along the polymer chains and form hydrogen bonds with the side groups of the outer layer, they cause internal friction of the intramolecular energy, resulting in a decrease in fluorescence. When the identified small molecules form a hydrogen bond directly on the pendant groups, they do not destroy the original hydrogen bond of the pendant polymer groups, as shown in Scheme 2B. In this case, the fluorescence intensity of the fluorescent polymer membrane will increase due to the electron donating effect of the identified small molecules, such as D-alanine and *S*-PEA, in this study. When there is no effect between the identified small molecules and the pendant groups of the polymer, the fluorescence intensity of the fluorescent membrane is not affected, as shown in Scheme 2C. We point out that the newly fabricated chiral nanofiber membranes have demonstrated some interesting phenomena, for which the exact reasons still remain to be explored. Nonetheless, based on the experiments and analyses above, we can draw a conclusion that the key factors affecting chiral recognition include two aspects. The first is the chiral helical structure of the polymer chains forming the fluorescent membrane. The second is the noncovalent interaction between a certain enantiopure chiral small molecule and the chiral fluorescent membrane. The chiral fluorescent nanofibers of this kind will be optimized in terms of the molecular structure, morphology, and functionality; besides chiral recognition, they will also be explored in chiral separation, asymmetric catalysis, *etc.* Studies

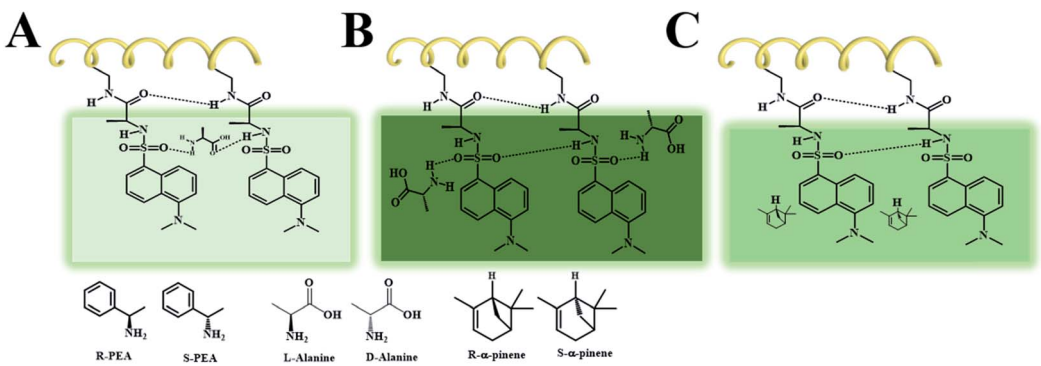

Scheme 2 The chiral recognition mechanism of the nanofiber membrane (L-PCMF): (A) mechanism of weakening fluorescence intensity; (B) mechanism of enhancing fluorescence intensity; (C) mechanism for the fluorescence intensity to keep constant.

 This journal is © The Royal Society of Chemistry 2020

Open Access Article. Published on 21 Februarie 2020. Downloaded on 2026-04-27 11:59:08 nm..
This article is licensed under a Creative Commons Attribution-NonCommercial 3.0 Unported Licence.

along these interesting directions may provide new insights into nano-scale chiral materials.

4. Conclusions

We have prepared chiral fluorescent polymer nanofiber materials by electrospinning technology. The L-PCMF chiral fluorescent membrane has fluorescence recognition for chiral amino acids (alanine) and chiral amines (phenylethylamine), while the D-PCMF chiral fluorescent membrane does not show such a recognition ability for chiral small molecules. The driving force for the chiral fluorescence recognition is proposed to be due to the hydrogen bonds formed between chiral small molecules and the pendant groups along the polymer chains. This study contributes the first success in preparing chiral fluorescent nanofiber materials from synthetic chiral helical polyacetylenes by the electrospinning technique. It also provides a new strategy for the design and preparation of new chiral fluorescent probes and even other chiral nano-materials.

Conflicts of interest

The authors declare no competing financial interest.

Acknowledgements

This work was supported by the National Natural Science Foundation of China (51973011 and 21774009).

Notes and references

1 M. Liu, L. Zhang and T. Wang, *Chem. Rev.*, 2015, **115**, 7304.
2 H. Huang, W. Li, Y. Shi and J. Deng, *Nanoscale*, 2017, **9**, 6877.
3 P. Li, K. Pan and J. Deng, *Nanoscale*, 2019, **11**, 23197.
4 E. Yashima, N. Ousake, D. Taura, K. Shimomura, T. Ikai and K. Maeda, *Chem. Rev.*, 2016, **116**, 13752.
5 L. C. Preiss, L. Werber, V. Fischer, S. Hanif, K. Landfester and Y. Mastai, *Adv. Mater.*, 2015, **27**, 2728.
6 W. Ma, L. Xu, L. Wang, C. Xu and H. Kuang, *Adv. Funct. Mater.*, 2019, **29**, 1805512.
7 Y. Zhao, A. N. Askarpour, L. Sun, J. Shi, X. Li and A. Alu, *Nat. Commun.*, 2017, **8**, 14180.
8 G. Vulugundam, S. K. Misra, F. Ostadhossein, A. S. Schwartz-Duval, E. A. Dazaa and D. Pan, *Chem. Commun.*, 2016, **52**, 7513.
9 G. K. E. Scriba, *J. Chromatogr. A*, 2016, **1467**, 56.
10 Y. Zhou, C. Zhang, R. Ma, L. Liu, H. Dong, T. Satohb and Y. Okamoto, *New J. Chem.*, 2019, **43**, 3439.
11 W. Liang, Y. Rong, L. Fan, W. Dong, Q. Dong, C. Yang, Z. Zhong, C. Dong, S. Shuang and W.-Y. Wong, *J. Mater. Chem. C*, 2018, **6**, 12822.
12 C. Pu, Y. Xu, Q. Liu, A. Zhu and G. Shi, *Anal. Chem.*, 2019, **91**, 3015.
13 Q. Wang, J. Huang, Z.-Q. Jiang, L. Zhou, N. Liu and Z.-Q. Wu, *Polymer*, 2018, **136**, 92.
14 N. Liu, C.-H. Ma, R.-W. Sun, J. Huang, C. Li and Z.-Q. Wu, *Polym. Chem.c*, 2017, **8**, 2152.
15 L. Zhang, Q. Jin and M. Liu, *Chem.–Asian J.*, 2016, **11**, 2642.
16 S. Arias, M. Núñez-Martínez, E. Quiñoá, R. Riguera and F. Freire, *Small*, 2017, **13**, 1602398.
17 H. Liu, Z. Li, Y. Yan, J. Zhao and Y. Wang, *Nanoscale*, 2019, **11**, 21990.
18 I. Fuchs, N. Fechler, M. Antonietti and Y. Mastai, *Angew. Chem., Int. Ed.*, 2016, **55**, 408.
19 L. C. Preiss, L. Werber, V. Fischer, S. Hanif, K. Landfester and Y. Mastai, *Adv. Mater.*, 2015, **27**, 2728.
20 Y. Zhang, Y. Wu, R. Xu and J. Deng, *Polym. Chem.c*, 2019, **10**, 2290.
21 S. H. Jung, J. Jeon, H. Kim, J. Jaworski and J. H. Jung, *Nanoscale*, 2015, **7**, 15238.
22 L. Dong, Y. Zhang, X. Duan, X. Zhu, H. Sun and J. Xu, *Anal. Chem.*, 2017, **89**, 9695.
23 J. Zou, X.-Q. Chen, G.-Q. Zhao, X.-Y. Jiang, F.-P. Jiao and J.-G. Yu, *Talanta*, 2019, **195**, 628.
24 M. E. McCarroll, F. H. Billiot and I. M. Warner, *J. Am. Chem. Soc.*, 2001, **123**, 3173.
25 Z.-Q. Jiang, S.-Q. Zhao, Y.-X. Su, N. Liu and Z.-Q. Wu, *Macromolecules*, 2018, **51**, 737.
26 N. Liu, H.-J. Lu, Z.-Q. Jiang, Y.-B. Lu, H. Zou, L. Zhou and Z.-Q. Wu, *Macromol. Chem. Phys.*, 2019, **220**, 1800574.
27 E. Yashima, N. Ousaka, D. Taura, K. Shimomura and T. Ikai, *Chem. Rev.*, 2016, **116**, 13752.
28 T. Miyabe, H. Iida, M. Banno, T. Yamaguchi and E. Yashima, *Macromolecules*, 2011, **44**, 8687.
29 X. Yong, Y. Wu and J. Deng, *Polym. Chem.c*, 2019, **10**, 4441.
30 S. J. Sahl, S. W. Hell and S. Jakobs, *Nat. Rev. Mol. Cell Biol.*, 2017, **18**, 685.
31 Y. Liu, C. Zhang, X. Li and D. Wu, *J. Mater. Chem. C*, 2017, **5**, 5939.
32 G. Beer, K. Rurack and J. Daub, *Chem. Commun.*, 2001, **12**, 1138.
33 Y. Xu and M. E. McCarroll, *J. Phys. Chem. A*, 2004, **108**, 6929.
34 Y. Yue, F. Huo, P. Ning, Y. Zhang, J. Chao, X. Meng and C. Yin, *J. Am. Chem. Soc.*, 2017, **139**, 3181.
35 M. Vendrell, D. Zhai, J. C. Er and Y.-T. Chang, *Chem. Rev.*, 2012, **112**, 4391.
36 S. Pandey, S. N. Baker, S. Pandey and G. A. Baker, *J. Fluoresc.*, 2012, **22**, 1313.
37 M. M. Green, J. -W. Park, T. Sato, A. Teramoto, S. Lifson, R. L. B. Selinger and J. V. Selinger, *Angew. Chem., Int. Ed.*, 1999, **38**, 3138.
38 R. Fasel, M. Parschau and K.-H. Ernst, *Nature*, 2006, **439**, 449.
39 H. Cao and S. D. Feyter, *Nat. Commun.*, 2018, **9**, 3416.
40 Y. Zhang, J. Deng and K. Pan, *Macromolecules*, 2018, **51**, 8878.
41 B. Zhao, K. Pan and J. Deng, *Macromolecules*, 2018, **51**, 7104.
42 H. Huang, W. Yang and J. Deng, *RSC Adv.*, 2015, **5**, 26236.
43 J. Xue, T. Wu, Y. Dai and Y. Xia, *Chem. Rev.*, 2019, **119**, 5298.
44 S. Jiang, Y. Chen, G. Duan and C. Mei, *Polym. Chem.c*, 2018, **9**, 2685.
45 T.-D. Lu, B.-Z. Chen, J. Wang, T.-Z. Jia, X.-L. Cao, Y. Wang, W. Xing, C. H. Lau and S.-P. Sun, *J. Mater. Chem. A*, 2018, **6**, 15047.

Open Access Article. Published on 21 Februarie 2020. Downloaded on 2026-04-27 11:59:08 nm..
This article is licensed under a Creative Commons Attribution-NonCommercial 3.0 Unported Licence.

46 M. J. Park, R. R. Gonzales, A. Abdel-Wahab, S. Phuntsho and H. K. Shon, *Desalination*, 2018, **426**, 50.
47 D. Li and Y. Xia, *Adv. Mater.*, 2004, **16**, 1151.
48 R. Gopal, S. Kaur, Z. Ma, C. Chan, S. Ramakrishna and T. Matsuura, *J. Membr. Sci.*, 2006, **281**, 581.
49 S. Zhang, Q. Shi, C. Christodoulatos, G. Korfiatis and X. Meng, *Chem. Eng. J.*, 2019, **370**, 1262.
50 M. W. Lee, S. An, S. S. Latthe, C. Lee, S. Hong and S. S. Yoon, *ACS Appl. Mater. Interfaces*, 2013, **5**, 10597.
51 Q. Wang, J. Ju, Y. Tan, L. Hao, Y. Ma, Y. Wu, H. Zhang, Y. Xia and K. Sui, *Carbohydr. Polym.*, 2019, **205**, 125.
52 S. K. Lim, S.-H. Hwang, D. Chang and S. Kim, *Sens. Actuators, B*, 2010, **149**, 28.
53 Q. Zhang, X. Wang, J. Fu, R. Liu, H. He, J. Ma, M. Yu, S. Ramakrishna and Y. Long, *Materials*, 2018, **11**, 1744.
54 R. R. Schrock and J. A. Osborn, *Inorg. Chem.*, 1970, **9**, 2339.
55 H. Yu, J. Liang and J. Deng, *Nanoscale*, 2018, **10**, 12163.

 This journal is © The Royal Society of Chemistry 2020